Informing Assistive Robots with Models of Contact Forces from Able-bodied Face Wiping and Shaving

Kelsey P. Hawkins, Chih-Hung King, Tiffany L. Chen, Charles C. Kemp

***Abstract*— Hygiene and feeding are activities of daily living (ADLs) that often involve contact with a person's face. Robots can assist people with motor impairments to perform these tasks by holding a tool that makes contact with the care receiver's face. By sensing the forces applied to the face with the tool, robots could potentially provide assistance that is more comfortable, safe, and effective. In order to inform the design of robotic controllers and assistive robots, we investigated the forces able-bodied people apply to themselves when wiping and shaving their faces. We present our methods for capturing and modeling these forces, results from a study with 9 participants, and recommendations for assistive robots. Our contributions include a trapezoidal force model that assumes participants have a target force they attempt to achieve for each stroke of the tool. We discuss advantages of this 3 parameter model and show that it fits our data well relative to other candidate models. We also provide statistics of the models' rise rates, fall rates, and target forces for the 9 participants in our study. In addition, we illustrate how the target forces varied based on the task, participant, and location on the face.**

I. Introduction

The aging population, rising healthcare costs, and shortage of healthcare workers in the United States create a pressing need for innovations that make personalized care more affordable and effective [1], [2]. Making contact with a care receiver's body is critical to many important caregiving tasks for people with physical disabilities. This is clearly illustrated by common definitions of activities of daily living (ADLs).

> "The term 'activities of daily living' refers to a set of common, everyday tasks, performance of which is required for personal self-care and independent living. [3]"

A person's ability to perform activities of daily living (ADLs) is predictive of his or her ability to live independently. ADLs include feeding, toileting, transferring, dressing, and hygiene [3]. Notably, each of these tasks typically involves contact with the care receiver's body. In order for robotic caregivers to physically assist with these critical tasks, they will very likely need to make contact with the user's body.

When a robot is in contact with a person's body, the contact forces become especially important due to considerations such as safety, comfort, and effectiveness at the task. This leads to the following question: What forces should robots apply to a care receiver's body when providing assistance? One approach to addressing this question is to use the forces that able-bodied people apply to themselves while performing tasks as a model for assistive robots. People have the ability to control the forces they apply, and receive feedback from both sides of each contact (i.e. feedback from the hand that is holding the tool and the location on the body where the tool is being used). As such, it is reasonable to assume that able-bodied people tend to apply forces to themselves that they find comfortable, safe, and effective. By emulating these forces, robots may also be perceived as applying forces that are comfortable, safe, and effective.

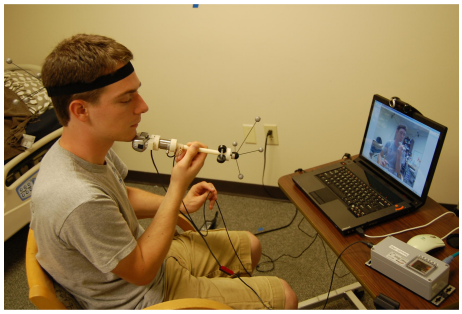

Fig. 1. **Shaving a Face Using a Handheld Tool:** A participant uses the handheld tool with an electric shaver fixture to shave his face. The laptop with the webcam allows him to view his face while performing the task.

Within this paper, we take this approach in the context of wiping and shaving. We first present our methods for capturing and modeling the contact forces that able-bodied people apply to themselves when wiping and shaving their faces. We then analyze the forces resulting from a study with 9 participants, and provide recommendations for the design of assistive robots based on this analysis. We selected wiping and shaving because they are relevant to hygiene, which is a type of ADL. Our results may also generalize to other types of robotic assistance since many tasks involve contact with a person's head (e.g., scratching an itch or blowing one's nose).

In section II, we discuss related research in force capture and analysis of safety for robots. We discuss our force capture system in section III, which consists of both a data capture studio and a procedure for registering the 3D data so that the results can be interpreted across multiple subjects. Section IV describes the study we ran to test the data capture system. In section V, we detail a technique for analyzing the stroke force using a trapezoidal model. We also investigate the positional dependence on force in section VI. Finally, we provide recommendations for assistive robots in section VII.

Healthcare Robotics Lab, Georgia Institute of Technology, Atlanta, GA, USA

[1]We obtained IRB approval and participant permission for all of the photos in this paper.

II. Related Work

Within this section, we discuss related research in characterizing forces and robotic safety.

A. Force Characterization

Redmond et al. collected forces and torques of subjects writing, opening/closing a jar, brushing teeth, and using a phone by instrumenting the devices [4]. They used root-mean-squared (RMS) statistics of the force magnitudes to characterize the distributions of recorded forces and to compare the tasks. To better understand the relationship between forces and the removal of plaque during toothbrushing, Van der Weijden et al. captured the forces of the task by having subjects use an instrumented toothbrush [5]. They measured the mean of the average individual force to be 3.2N$\pm$1.1N. Wells and Greig analyzed the forces and moments of holding objects like power drills and screwdrivers by describing the situation geometrically, though they did not collect forces during use [6]. Force statistics in haptic interactions have also been collected in surgical tasks [7], as well as stair climbing and sit-to-stand transitions [8]. Previously we have captured the motions and forces associated with opening doors and drawers using a portable force and motion capture system [9] [10].

B. Robotic Safety

Research has also been conducted to characterize the physical dangers associated with robotics systems. The majority of severe accidents involving industrial robotics technology, which tends to be heavier, more powerful, and less tailored to human interaction than the robot used in our research, involve crushing of a victim by the robot against a fixed object, often when the operator was alone, and only 20% occurred during normal operation [11]. A number of groups, including the International Standards Organization (ISO) [12], have sought to establish guidelines for the design and control of safe robots for human interaction [13]–[16]. In particular, Haddadin et al. examined the potential for injury from a lightweight 7-DoF robot arm using a standardized crash test dummy in unconstrained blunt impacts, and porcine cadavers in cutting and stabbing impacts [17]. By examining the force required to cause fractures in both weak and strong bones in the face (660 N to 4000 N), they found that velocities between 0.5 and 1.0 m/s could be dangerous, even for robots with 5 kg of reflected inertia. A significant potential for injury is posed by sharp impacts, though they were able to mitigate this danger using active collision detection and reaction with their robot arm [18].

III. Implementation

In this section we discuss our setup and process for collecting force data.

A. Data Capture Studio

We used an OptiTrack infrared optical motion capture system to track the 6-axis position and orientation of objects instrumented with four reflective markers. A set of these markers was attached to a handheld tool along with a force/torque sensor so we could track the force and position of contact when used by a person to perform ADL tasks (Fig. 2). The tool handle and adapter plates are fabricated from plastic using a 3D printer. A modular design allows us to create tools for various ADL tasks by attaching different tool heads using screws (Fig. 2). We sample force/torque sensor data at 100 Hz.

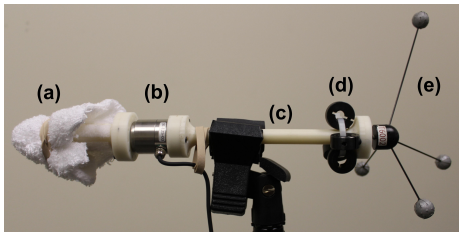

Fig. 2. **A handheld tool for ADL task data collection:** (a) ADL tool head (shown here is a face wiping tool covered with washcloth). (b) Six-axis force/torque sensor (ATI Nano25-IP65). (c) Handle. (d) Counter weight. (e) Tracking target.

Using the orientation of the tool provided by the motion capture system, we compensated for gravity by subtracting out the force vector exerted by the head of the tool on the force sensor. We found that strain on the force sensor would, over time, offset the center of the force readings by a constant amount. To account for this effect, we biased the sensor at the beginning of each trial relative to the force reading of the sensor when the tool is motionless.

We also capture and reconstruct a 3D representation of the participant's head. A tracking target is rigidly attached and registered to a Kinect (Microsoft) sensor and mounted on a wheeled tripod (Fig. 3). This setup allows us to quickly and stably move the sensor around the participant to collect different perspectives of his or her face in the same global frame. We also attach a tracking target to the participant's head using a head band. Although the relative motion of the participant's head is available, the location of the tracker and head band was not controlled.

To get a reconstruction of the subject's full head in 3D, we collect point clouds from eight positions all around the participant's head. Each point cloud is transformed into the head tracker's frame and the background is removed based on the location of the points with respect to the head tracker. Since the error in the Kinect's calibration is relatively large, we use a feature-based registration technique for more accurate splicing (Alg. 1). Starting with the cloud from the front-face perspective, each successive cloud is registered and concatenated to the full cloud. The three clouds on the right side of the face are registered first, followed by the left three, and finally the back. Overlaps between successive clouds are found by finding all points in each cloud within 3cm of the points in the other. The iterative closest point (ICP) algorithm is used to find the transformation between the overlapping clouds where the distance metric includes both point distances and color distances in HSV space.

Algorithm 1 HEADRECONST($pc^{front}, \{pc_i^{left}\}, \{pc_j^{right}\}$)

$pc^{full} \leftarrow pc^{front}$
for pc_i^{left} in $\{pc_i^{left}\}$ **do**
  $pc_{ol}^{left}, pc_{ol}^{full} \leftarrow$ FINDOVERLAP(pc_i^{left}, pc^{full})
  $B_{reg} \leftarrow$ ICP($pc_{ol}^{left}, pc_{ol}^{full}$)
  $pc_{reg}^{left} \leftarrow$ TRANSFORM(pc_i^{left}, B_{reg})
  $pc^{full} \leftarrow pc^{full} + pc_{reg}^{left}$
end for
// Repeat for $\{pc_j^{right}\}$
return pc^{full}

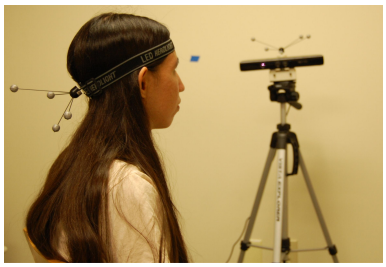

Fig. 3. **Capturing 3D Point Clouds of a Participant's Head:** Moving a Kinect sensor around a participant to collect 3D point clouds. [1] The pose of the Kinect and the pose of the participant's head are tracked using the mounted tracking targets.

B. Data Registration

Although the positions of the tool at any point in time can be found consistently with respect to the head tracker's frame, the rigid transformation between the tool tip position and the head reconstruction often shows an error of a 1-3cm due to poor registration and/or error in the reconstruction. To reduce this error we first created a point cloud of contact locations for reference. We processed the force-position data to form a point cloud representing the location of the tool tip at all times the force magnitude is greater than 0.5N. We manually register this cloud for each subject to a model head reconstruction using a 6-DOF click-and-drag interface which allows us to position and rotate it to find the rigid transformation. We use the curvature and extent of the contact cloud as a reference for lining it up to the model's cloud. Each point is then projected to the closest point in the head reconstruction of the model. This last transformation keeps poor registration from resulting in low weights in the regression.

IV. EXPERIMENTAL DESIGN

We conducted an experiment with able-bodied students to capture the force distributions they apply when performing two types of ADL tasks: wiping debris off their faces and shaving their faces. We recruited 9 students (male=4, age=20-25) from the Georgia Tech campus through email lists and word of mouth. The male participants performed the shaving task prior to the wiping task, and the female participants performed the wiping task only. We required participants to be at least 18 years of age and to speak English fluently. The self-reported ethnicity of these participants were Caucasian (6), African American (1), and other (2).

For both tasks, we asked each participant to use his or her dominant hand to hold the tool in whatever manner was comfortable. Since a normal mirror may reflect the IR light emitted from the IR cameras and may interfere with the optical tracking system, we placed a laptop with a webcam (Logitech Webcam Pro 9000) in front of the participant so he or she could see his or her face (Fig. 1). Before they began, the experimenter asked the participant to hold the tool about an inch away from his face and called this the "start position". The task began when the experimenter said the word "begin". We asked the participant to verbally tell us when they were finished and to hold the tool back at the starting position. We did not impose a time limit because we wanted the participant to use the amount of time they might normally take.

A. Shaving Task

In the shaving task, we asked the male participant to use an electric shaver (approximate contact area: 2.9cm x 5.6cm = 16.2cm^2) attached to the handheld tool to shave his face. Before each experiment began, we placed a brand new set of shaver blades on the shaver head. We also cleaned and sanitized the cover and the shaver head using Barbicide wipes (King Research, Milwaukee, WI). The experimenter asked the participant to shave how he normally would have if he had used a tool similar to the handheld tool (Fig. 1).

B. Wiping Task

In the wiping task, we asked the participant to use a moist towel attached to the handheld tool to remove talcum powder from an area of his or her face. The plastic base of the wiping head was inspired by two fingers held together side by side (approximate contact area: 2.3cm x 3.7cm = 8.5cm^2). We asked the participant to use his or her dominant hand to perform the task. To simulate debris, we applied talcum powder to an area of the participant's face. We selected talcum powder since it is commonly used in personal hygiene and cosmetics, and it does not leave stains on the skin after being wiped off. We selected the side of the face on the same side of his or her dominant hand. We used a new cosmetic sponge to apply the powder to the participant's face and provided a new face mask to prevent inhalation of the powder. For each participant we attached a new towel to the wiping tool using a new rubber band and moistened the towel before each trial.

We asked the participant to mimic how they might normally clean the area of the face using a similar tool until there is visibly no more powder remaining (Fig. 4). While users do not generally use such devices to wipe their faces, the user does have control over the force applied by the tool to his or her face and we designed the tool to emulate a piece of cloth wrapped around two fingers.

C. Procedure

We performed our experiment in the Healthcare Robotics Lab in a 4.3m x 3.7m room. Two experimenters (the second

Fig. 4. **Wiping a Face Using a Handheld Tool:** A participant uses the handheld tool with a moist towel to remove the talcum powder on his face. In this task he is removing the powder on his cheek.

Fig. 5. **Talcum powder regions:** We applied talcum powder to the cheek, chin, and nose before the wiping trials began.

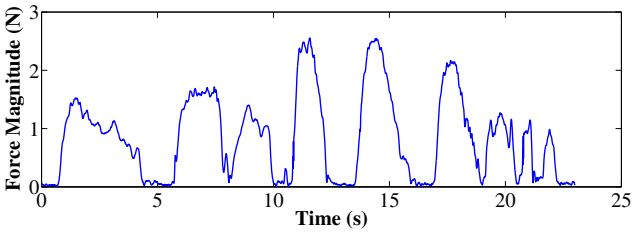

Fig. 6. **Wiping Force Profile:** Force magnitudes of a subject during a full wiping trial of the cheek with the handheld tool.

and third authors of this paper) conducted all of the trials and remained in the room throughout the experiment to ensure the participant's safety. One experimenter proctored the experiment by reading a script. The participant was first welcomed to the lab and introduced to the experimenters. Then the participant was asked to sign a consent form, fill out a demographic survey, and fill out a pre-task questionnaire.

The experimenter then asked the participant to sit at a chair which had been placed at a fixed location. The experimenter asked the participant to affix a tracking target to his or her head using a specially designed headband. They were asked not to touch or move the headband or the tracking target during the entire experiment. To collect data for the 3D head reconstruction discussed in section III-B, we captured 3D point cloud data at eight positions around the participant. During the process of capturing the point cloud data, the experimenter asked the participant to sit still and keep a neutral facial expression. Afterward, the experimenter explained the use of the tool to perform the ADL task.

During recruitment we asked the male participant not to shave his face 24 hours prior to the appointment time of the experiment, and to bring the shaving tools they normally would use to shave his face. At the end of the shaving task, we asked the participant to go to the rest room and finish shaving his face using the tools he brought with them. Each participant performed a practice trial to allow themselves to get comfortable using the handheld tool and the test procedure. We kept a sanitized plastic cover on the shaver during practice. Each male participant performed the shaving task once.

We asked all participants to perform the wiping task three times. Before they began any of the three tasks, we put talcum powder on both the cheek, nose, and the chin of the participant's face. In each trial asked them to wipe the talcum powder off only one of the three regions. We counter balanced the ordering of the trials across participants prior to data collection.

V. A Trapezoidal Model of Stroke Force

We have analyzed the data produced in the experiment to characterize the forces involved in the tasks and the sources of variance. Figure 6 illustrates that participants, when wiping the face, generally break the task down into a series of strokes. For our analysis, we identified the beginnings and endings of these strokes using a contact threshold of 0.5 N and discarded all strokes shorter than 0.2s in duration.

The shapes of the strokes are similar across both the individual's strokes and across users: contact is made, the force ramps up, the force fluctuates at a consistent level, and then it ramps down. To quantify this structure, we have created a trapezoidal model of the magnitude of the contact force in a stroke. It models these three regimes using a piecewise linear function of time. The middle regime is defined by a constant force magnitude. For our model, we assume that the person attempts to achieve this force magnitude during the stroke, and thus refer to it as the *target force*, f_t.

Mathematically, we define our model as

$$f^{trap}(t) = \begin{cases} (f_t - 0.5)\frac{t}{t_r} + 0.5 & t \leq t_r \\ f_t & t_r \leq t \leq t_f \\ (f_t - 0.5)\frac{t - t_{end}}{t_f - t_{end}} + 0.5 & t > t_f \end{cases} \quad (1)$$

where the parameters are illustrated in Figure 7.

In order to fit our trapezoidal model to stroke data, we perform a nonlinear least squares fit. The fit is performed by first sampling over a uniform distribution of initial values for the three model parameters (f_t, t_r, t_f). For each seed triple, a

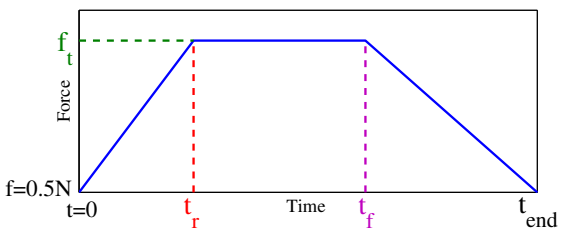

Fig. 7. **Trapezoidal Model:** An illustration of the parameters fit to each stroke. The three parameters are the target force f_t, the rise time t_r, and the fall time t_f.

nonlinear curve-fitting optimization technique is used to find a local optimum least-squares fit (*lsqcurvefit* in Matlab). The best fit over all initial conditions is chosen as the parameters for that particular stroke. We fit a trapezoidal model to every stroke for each subject for each of the three wiping tasks and the shaving task. Our model fixes the bottom corners of the trapezoid to the beginning and ending of each stroke at 0.5 N.

A. Model Advantages

Modeling each stroke using a trapezoidal model presents several advantages over other modeling methods. First, the target force has a clear interpretation for robots, since it can be used as a reference force for a robot's force controller. Similarly, ramping up can be related to the rise time of a robot's force controller. Second, the model captures salient properties of each stroke that can be hidden with other models. For example, modeling the raw force magnitudes using a single distribution conceals the time structure of each stroke and the contribution of individual strokes. It is also not conducive to interpretation as having a *target force*, since ramping up and down biases the distribution and summary statistics to lower values. Likewise, principal component analysis (PCA) does not lead to a clear interpretation in terms of target force, since each basis function represents the entire stroke. Third, this 3-parameter model has a comparatively good fit to the force magnitudes from our experiment. Figure 11 illustrates how this technique models the original data.

B. Fitting Error

We report mean squared error (MSE) for the trapezoidal fit in Table V-C, and also compare it to the MSE for other reconstruction techniques. The largest MSE is 0.14 for shaving, which is a small error relative to the shaving forces and the measurement capabilities of our force-torque sensor.

We compared this fitting error to using a horizontal line centered at the mean value of each stroke (mean line model), and two low-dimensional PCA models. For the PCA models, we took all strokes for a given task, resampled them to create 100 dimensional vectors, and then performed PCA. We report MSE for a PCA model with 2 components and 3 components. Figure 8 shows the mean and top PCA components for the cheek wiping task.

	Wiping			
	Cheek	Chin	Nose	Shaving
Minimum (N)	0.59	0.59	0.56	0.55
Lower quartile (N)	1.56	1.33	1.29	0.89
Median (N)	2.39	1.98	1.92	1.89
Upper quartile (N)	3.14	2.70	3.21	2.68
Maximum (N)	5.45	5.37	7.75	8.20

TABLE I

STATISTICAL CHARACTISTICS OF TARGET FORCES ACROSS SUBJECTS, EXCLUDING SUBJECT 9.

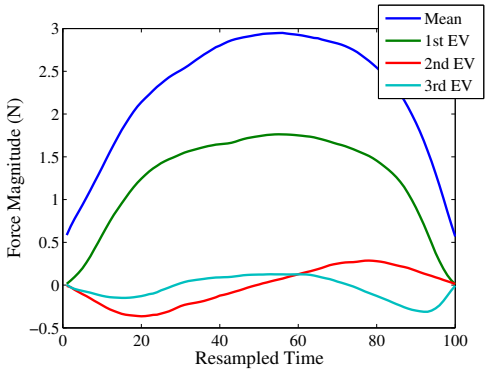

Fig. 8. **PCA Analysis:** The mean and top three eigenvectors (EV) from the PCA performed on resampled strokes for the cheek wiping task. Since the eigenvectors are unitless, we scaled them relative to each other by multiplying by the corresponding singular values, then uniformly by a constant to bring them into the same scale as the mean.

The trapezoidal model fit our data an order of magnitude better than the mean line model. It fit better than the 2 component PCA model, but not as well as the 3 component model.

C. Statistics for the Trapezoidal Model Parameters

Table V-C also reports the rise and fall rates which are computed by dividing the target force by the rise and fall times.

Figure 9 provides a statistical characterization of the distribution of target forces across the strokes across all users. We treat subject 9 as an outlier for the wiping tasks and excluded his data in the overall statistics, since subject 9's forces far exceeded the distributions for the other eight subjects.

VI. FORCE CONDITIONED ON FACIAL LOCATION

We have also investigated the relationship between force and position on the face. As Fig. 9 shows, the variance in forces across users is far greater than the variance within each user. In order to reduce this population-wide variance, we divide each participant's force data by the mean of his or her target forces. We then use this normalized force magnitude $\hat{f}$ to find the expected force magnitude at each point p on the face $\mathbf{E}[\hat{f}|p]$.

	Wiping			
	Cheek	Chin	Nose	Shaving
MSE 3D PCA (N^2)	0.04	0.03	0.06	0.11
MSE trapezoidal (N^2)	0.06	0.04	0.11	0.14
MSE 2D PCA (N^2)	0.08	0.09	0.15	0.20
MSE mean line (N^2)	1.30	0.61	1.35	0.61
Mean rise rate (N/s) (Standard deviation)	13.3 (10.8)	12.3 (8.7)	11.4 (6.7)	9.8 (6.7)
Mean fall rate (N/s) (Standard deviation)	12.0 (15.7)	8.3 (13.5)	14.1 (17.9)	11.4 (13.3)
Mean strokes count (Standard deviation)	15.1 (6.6)	9.4 (5.0)	12.8 (5.4)	81.5 (32.1)
Mean stroke duration (s) (Standard deviation)	0.96 (0.61)	0.94 (0.60)	0.77 (0.51)	1.67 (2.38)

TABLE II

EXTRA TRAPEZOID MODEL FITTING STATISTICS.

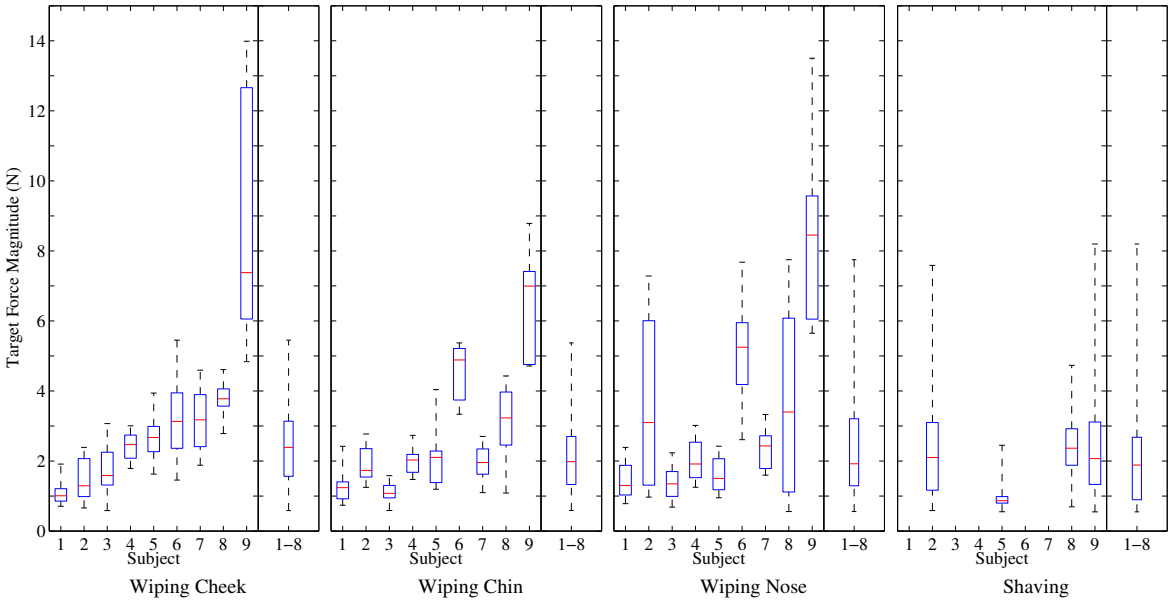

Fig. 9. **Target Force Distributions:** Box plots of the minimum, maximum, median, and quartiles of stroke target forces for each subject, for each task. The boxes on the left for each task characterize the distribution of trapezoid heights for each subject. The box on the right for each task is a summary of the across-subject distribution, excluding subject 9. This distribution is normalized by resampling the number of each subject's forces to an equal number so as to eliminate per-subject bias. Subjects are sorted by the median target force of the wiping cheek task.

$$\mathbf{E}[f^*|p] = \int \hat{f}\,\mathbf{P}(\hat{f}|p)\,d\hat{f} \tag{2}$$

$$\mathbf{P}(\hat{f}|p) = \frac{\sum_u \mathbf{P}(\hat{f},p,u)}{\sum_u \mathbf{P}(p,u)} \tag{3}$$

We use non-parametric kernel density estimation to compute the regression, similar to the Nadaraya-Watson estimator [19]. An important modification is required because each participant's data set should be weighed equally. Equation 3 shows how we reintroduce the nominal participant variable u by marginalizing it out. Factoring the probabilities and using a kernel density estimate to model them, we are left with

$$\mathbf{E}[\hat{f}|p] = \frac{\sum_u \frac{1}{N(u)} \sum_{(p_i,\hat{f}_i)\in\mathbb{D}(u)} \hat{f}_i\, K_p(p-p_i)}{\sum_u \frac{1}{N(u)} \sum_{(p_i,\hat{f}_i)\in\mathbb{D}(u)} K_p(p-p_i)} \tag{4}$$

$$K_p(p-p_i) = \exp(-\frac{1}{2}\frac{||p-p_i||^2}{h_p^2}) \tag{5}$$

where K_p is the standard squared exponential kernel and h_p is a kernel bandwidth parameter. The inner sums iterate over the set of data pairs

$$\mathbb{D}(u) = \{(p_i,\hat{f}_i) \mid ||p-p_i||^2 < 3h_p,\ \hat{f}_i \geq 0.5\} \tag{6}$$

The term $\frac{1}{N(u)}$ weighs each participant's contribution to the regression equally by dividing by the number of data points from his or her data set. Using the dimensions of the tools as a reference, we set the bandwidth parameter to $h_p = 2$cm.

The prior probability on the position distribution is proportional to the denominator of (4).

$$\mathbf{P}(p) \propto \sum_u \frac{1}{N(u)} \sum_{(p_i,\hat{f}_i)\in\mathbb{D}(u)} K_p(p-p_i) \tag{7}$$

This unitless distribution indicates relatively where contact is being made more frequently. In the figures, points with low frequency ($\mathbf{P}(p_{low}) \leq 0.5 \max_p[\mathbf{P}(p)]$) are not colored

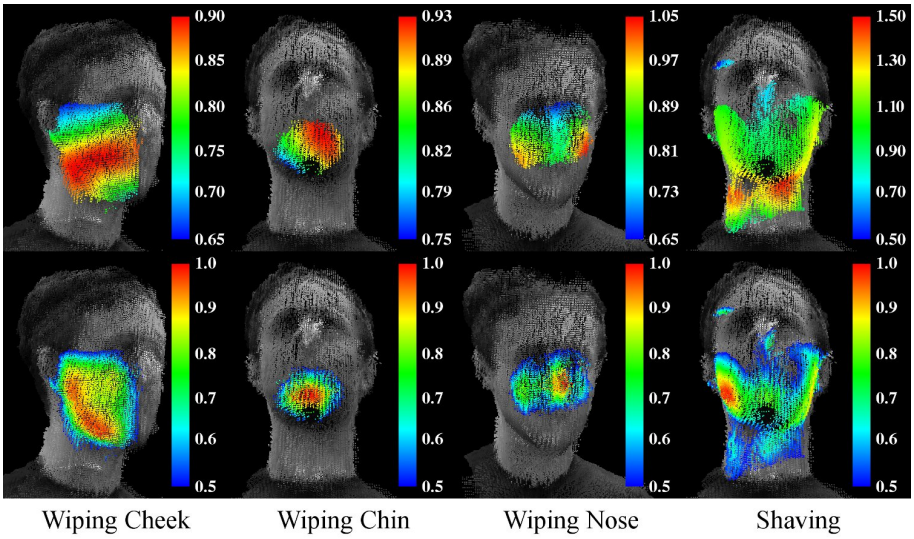

Fig. 10. **Force Dependence on Position: Top**: Expected value of normalized force magnitude across all users at a given point on the face $\mathbf{E}[\hat{f}|p]$. Forces are all normalized using the means of the target forces. This means a value of 1.0 corresponds to the mean target force for each subject. **Bottom**: Distribution of contact forces $\mathbf{P}(p)$. A red hue indicates regions where subjects made contact with for the most amount of time while a blue hue indicates regions where the time was half of the time spent in the red regions.

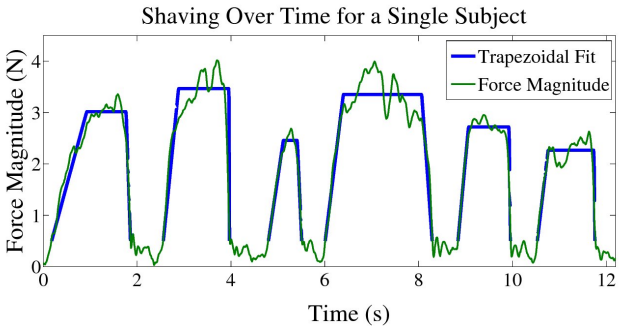

Fig. 11. **Trapezoidal Fit:** Models have been fit to each of the swipes in this excerpt of a shaving force profile.

so as to eliminate smoothing at the boundaries. Figure 10 presents the results of the density estimation.

VII. Recommendations for Assistive Robots

We have motivated this investigation with the idea that robots could use our models to better interact with humans. Within this section, we discuss ways in which our results can be used by assistive robots and designers of assistive robots.

A. Customization and Control of Forces

The distributions of target forces for some subjects were distinctly different from others (Fig. 9). The variance in many distributions is relatively small and some distributions do not overlap with one another. Since we carefully controlled the wiping task, some of this variation is likely due to personal preference, rather than task requirements. These results suggest that people might prefer assistive robots that enable them to tune contact forces to their personal preferences.

B. Rise and Fall Rates

Using the rise and fall rates presented in Table V-C, a force controller could attempt to track a trapezoidal force profile as it strokes with a tool across the face. We found statistical significance ($p < .001$) that the rise rate across all strokes for wiping is greater than the rise rates for the shaving task. This might suggest that people were more careful when increasing the force of the razor than they were when pulling the razor away and using the wiping tool. Emulating this type of capability depending on the task may also be desirable in assistive robots.

C. Varying Force Based on Location

Figure 10 indicates that the applied forces varied in consistent ways with respect to the contact location on the person's face. For example, when wiping the cheek, subjects applied lower forces near the top of the check next to the eyes. Also, individuals applied lower forces along the bridge of the nose compared with the sides of the nose. When shaving, subjects tended to apply more force to the region of the neck underneath the chin than to the cheek and jaw bone. The position distributions reveal that individuals spent more time along the jaw bone and the bridge of the nose when wiping and shaving. Robots could potentially use this type of information to avoid making contact or applying high forces to irrelevant or sensitive locations, such as the eyes during shaving. The extent to which more nuanced variation in the force would be beneficial is an open question.

Also, we did not control for different face geometries. As a result, the locations of the nose, ears, and other facial features might be slightly different across subjects in the data. However, we believe the extent of the error added does not detract significantly from our results, since the smoothing

Fig. 12. **Robotic Shaving with Force Sensing:** Henry Evans shaves himself with a Willow Garage PR2 robot. In this test, the subject was able to obtain nicks and abrasions, motivating the need for intelligent force sensing.

parameters in the density estimation are likely larger than the error in face correspondence.

D. Maximum Forces

The maximum target forces provide evidence about the forces that are sufficient to perform the tasks and the range of forces that are comfortable. Robot designers could use these forces as guidelines for the forces that an assistive arm should be able to apply. Robots could also restrict the forces they apply during a task. Figure 9 shows that for the inliers, the target forces for all tasks fall at or below 8.2 N. The extent to which these forces generalize to other tasks, tools, and people remains an open question that merits further research.

E. An Example Using a Force Threshold

Our work has been motivated in part from the Robots for Humanity project, a collaboration between the Georgia Tech Healthcare Robotics Lab, Willow Garage, Prof. Bill Smart, and Henry Evans. As part of this project, we have developed an assistive shaving system for the Willow Garage PR2 robot that Henry Evans, who has quadriplegia, has used to shave his cheek and chin (see Figure 12). In his first test of this system, Henry abraded and nicked his skin. We recorded the forces during this test, and found that he was applying high forces to his face ($\sim$ 25N). We then developed a behavior which would back the arm away from his face if the force exceeded a threshold of 10N. We based this threshold on a pilot study of able-bodied people shaving that used methods similar to the methods in the current paper. In a test of this new system, Henry triggered this threshold a few times, but adapted his use of the system to mostly stay below the threshold while performing the task. He successfully shaved his cheek and chin, but did not abrade or nick his skin in the process. Our results in the current paper further support 10N as a reasonable threshold, and we have continued to use it during more recent tests.

Our experience to date suggests that modeling the contact forces applied by able-bodied users during tasks can usefully inform the design of assistive robots and their behaviors. This approach has the potential to improve the safety, comfort, and effectiveness of assistive robots, and, hence, the lives of people with motor impairments.

VIII. Acknowledgments

We thank Phillip M. Grice, Marc Killpack, and all the participants. We gratefully acknowledge support from Willow Garage, the National Science Foundation (NSF) Graduate Research Fellowship Program, and NSF grants CBET-0932592, CNS-0958545, and IIS-0705130. We also thank the team members of the Robots for Humanity Project with special thanks to Henry Evans.

References

[1] Institute of Medicine, *Retooling for an Aging America: Building the Health Care Workforce*. The National Academies Press, 2008.

[2] H. J. Goodin, "The nursing shortage in the united states of america: an integrative review of the literature," *J Adv Nurs*, 2003.

[3] J. M. Wiener, R. J. Hanley, R. Clark, and J. F. V. Nostrand, "Measuring the activities of daily living: Comparisons across national surveys," *Journal of Gerontology: SOCIAL SCIENCES*, vol. 45, no. 6, pp. S229–237, 1990.

[4] B. Redmond, R. Aina, T. Gorti, and B. Hannaford, "Haptic characteristics of some activities of daily living," in *Haptics Symposium, 2010 IEEE*, 2010, pp. 71 –76.

[5] G. V. der Weijden *et al.*, "Relationship between the plaque removal efficacy of a manual toothbrush and brushing force," *J. Clin. Periodontol*, vol. 25, pp. 413–6, 1998.

[6] R. Wells and M. Grieg, "Characterizing human hand prehensile strength by force and moment wrench." *Ergomonics*, vol. 44, no. 15, pp. 1392–1402, 2001.

[7] J. Rosen *et al.*, "Surgeon/endoscopic tool force-torque signatures in the evaluation of surgical skills during minimally invasive surgery," January 1999.

[8] A. Erdemira *et al.*, "Model-based estimation of muscle forces exerted during movements," *Clin. Biomech.*, vol. 22, no. 2, pp. 131–154, 2007.

[9] A. Jain *et al.*, "The complex structure of simple devices: A survey of trajectories and forces that open doors and drawers," in *IEEE Int. Conf. Biomed. Robo. and Biomech.*, 2010.

[10] A. Jain and C. C. Kemp, "Improving robot manipulation with data-driven object-centric models of everyday forces," *Under Review 2012*.

[11] T. Malm, J. Viitaniemi, J. Latokartano, S. Lind, O. Venho-Ahonen, and J. Schabel, "Safety of interactive robotics – learning from accidents," *Int J Soc Robot*, vol. 2, pp. 221–227, May 2010.

[12] C. Harper and V. Gurvinder, "Towards the development of international safety standards for human robot interaction," *Int. J. Soc. Robot*, vol. 2, pp. 229–234, Jun. 2010.

[13] J. Heinzmann and A. Zelinsky, "Quantitative safety guarantees for physical human-robot interaction," *Int. J. of Robotics Research*, vol. 22, pp. 479–504, Jul. 2003.

[14] K. Ikuta, H. Ishii, and M. Nokata, "Safety evaluation method of design and control for human-care robots," *Int. J. of Robotics Research*, vol. 22, no. 5, pp. 281–297, May 2003.

[15] M. Guiliani, C. Lenz, T. Muller, M. Rickert, and A. Knoll, "Design principles for safety in human-robot interaction," *Int. J. Soc. Robot*, vol. 2, pp. 253–274, Mar. 2010.

[16] Y. Yamada, Y. Hirasawa, S. Huang, Y. Umetani, and K. Suita, "Human-robot contact in the safeguarding space," in *IEEE/ASME Transactions on Mechatronics*, vol. 2, no. 4, Dec. 1997, pp. 230–236.

[17] S. Haddadin, A. Albu-Schaffer, and G. Hirzinger, "Safety analysis for a human-friendly manipulator," *Int J Soc Robot*, vol. 2, pp. 235–252, May 2010.

[18] G. Sami Haddadin, Alin Albu-Schaffer, "Soft-tissue injury in robotics," in *IEEE Int. Conf. on Robotics and Automation (ICRA2010)*, Anchorage, Alaska, USA, May 2010.

[19] B. Hansen, "Nonparametric regression," *Lecture*, 2009. [Online]. Available: http://www.ssc.wisc.edu/~bhansen/718/NonParametrics2.pdf